Materials Research Proceedings 41 (2024) 40-49 https://doi.org/10.21741/9781644903131-5

Prediction of the evolution of material properties during the AM process based on the FEM simulation and experimental results

HÄRTEL Sebastian[1 a*], SZYNDLER Joanna[1,b], PAKDEL SEFIDI Moein[1,c] and JÄGER Reyk[1,d]

[1]Chair of Hybrid Manufacturing, Brandenburg University of Technology, Cottbus, Germany

[a]haertel@b-tu.de, [b]Joanna.Szyndler@b-tu.de, [c]pakdelse@b-tu.de, [d]Reyk.Jaeger@b-tu.de

Keywords: Finite Element Method (FEM), Wire Arc Additive Manufacturing (WAAM), Additive Manufacturing AM, Material Properties

Abstract. To deepen the understanding of material behavior after additive manufacturing, this article focuses on the prediction of material properties after the Wire Arc Additive Manufacturing (WAAM) process. Particular attention is put on the temperature curves in the various phases of the welding process, which influence the final material properties, especially the hardness of the resulting part. A total of nine components in the form of walls were produced using the WAAM process, with the number of layers varying from 1 to 9. By experimentally analyzing the welded parts, which were cut in the middle of their length, it was possible to gain insights into the development of hardness at selected points. The entire test setup was simulated in the Simufact Welding FE-software. The simulation results in the form of temperature-time diagrams were then correlated with the real hardness measurements at the corresponding points. In this way, a model was developed that for the first time considers the development of hardness as a result of cooling after the welding process as well as the change in hardness as a result of reheating due to the application of additional layers.

Introduction

A revolutionary manufacturing technique called additive manufacturing has the power to completely transform a wide range of industry sectors. Complex geometries that are challenging or impossible to create using conventional manufacturing techniques can be fabricated using additive manufacturing. However, predicting the final material properties of the additively manufactured parts is one of the challenges. The geometry of the object, the printing parameters, and the kind of material being used are just a few of the many variables that can make Additive Manufacturing (AM) a complex process. All of these elements may have an impact on the printed part's ultimate properties like strength, hardness, and ductility. Predicting material properties during and after the additive manufacturing process would enable process optimization and the creation of parts with desirable properties. For the fabrication of high-performance parts for crucial applications, this would be especially advantageous.

Bai, Y., et al. predicted how residual stresses in additively manufactured parts would change using FEM simulation [1]. Machine learning was used by Zhao, Y., et al. to forecast the mechanical characteristics of additively manufactured parts, such as their ductility and strength. The relationship between the properties of the printed part and the initially used material can be discovered by training machine learning algorithms with experimental data [2]. Wu, S., et al. looked into the connection between the mechanical characteristics and microstructure of Ti-6Al-4V that was additively manufactured. A common titanium alloy used in AM applications is Ti-6Al-4V. The microstructure of Ti-6Al-4V and additively manufactured Ti-6Al-4V differs significantly, according to the study. The material's mechanical properties may be significantly impacted by this variation in microstructure [3]. A multi-scale method for forecasting the fatigue

behavior of additively manufactured parts was created by Zhang, B., et al. This study developed a multi-scale approach to predict the fatigue behavior of an additively manufactured part by considering its microstructure, defects, and stress distribution [4]. A prediction model for the final properties of AlSi10Mg parts made by additive manufacturing was created by Li, Y., and colleagues. An aluminum alloy that is frequently utilized in AM applications is AlSi10Mg. To predict the properties of the additively manufactured part, the study's predictive model considers both its microstructure and printing parameters [5]. A substantial body of prior research serves as the basis for this study, which predicts how material properties will change during the additive manufacturing process. The integrated method presented here enables the prediction of long-term changes in material properties by combining experimental data and FEM simulations. The model can be used to make the AM process more efficient and consistent so that parts are produced with the expected quality.

In this research, a Finite Element (FE) model of the AM process is developed to predict the material properties during the process with an analytical model. The part geometry, material, and welding parameters are included in the FE model. The temperature history in the component is then calculated and the hardness development due to cooling after the layer has been deposited and reheating by depositing new layers is calculated using the analytical model.

Workflow of the investigation

This study presents a model that is developed to predict the final hardness distribution of a structural steel component produced by Wire Arc Additive Manufacturing (WAAM). The proposed model postulates that the final hardness (HV_{final}) decreases due to reheating by welding additional layers and the resulting thermal energy input ($E_{thermal}$). The specific decrease in hardness is represented by (ΔHV). A further assumption concerns the influence of the cooling rate $\dot{T}$ of a newly applied layer, which influences the initial hardness (HV_{ini}). It is assumed that the application of new layers using WAAM leads to a reduced initial hardness due to a slower cooling rate. This is because the already existing component acts like a "thermal battery" due to the higher temperature and thus reduces the cooling rate of the newly applied layer. Based on these assumptions, this article aims to define a method for determining the final hardness HV_{final} of a part designed with WAAM using FE simulation including the following equation:

$$HV_{final} = HV_{ini}\left(\mathrm{F}\left(\dot{T}_{800-500}\right)\right) - \Delta HV(\mathrm{F}(E_{thermal}) \quad (1)$$

To determine the influence of the cooling rate on the initial hardness, straight walls with 1 to 9 layers were welded experimentally. The hardness of the upper seam was then measured. The analysis of the upper seam has the advantage that the resulting hardness is only influenced by the cooling rate and not by reheating, as no further layer is applied. For walls built of several layers, the next layer was applied with a fixed break time of 38 seconds. The numerical simulation of nine walls with 1 to 9 layers was then conducted. Here, the cooling rate between 800 and 500 °C was determined in the upper seam. Using the measured hardness values of the top layer and the calculated cooling rates, a mathematical description coupling the resulting hardness and cooling rate can be made according to notation. 2.

$$HV_{ini}\left(\mathrm{F}\left(\dot{T}_{800-500}\right)\right) \quad (2)$$

The basic procedure is shown in Fig. 1a. In addition, a wall with nine layers was produced using the WAAM method and simulated (see Fig. 1c).

A summary of the general procedure for developing a physically based model from experimental measurement data (hardness) and simulation data, which can be used to predict the hardness distribution of a component after the WAAM process through process simulation is presented in Fig. 1.

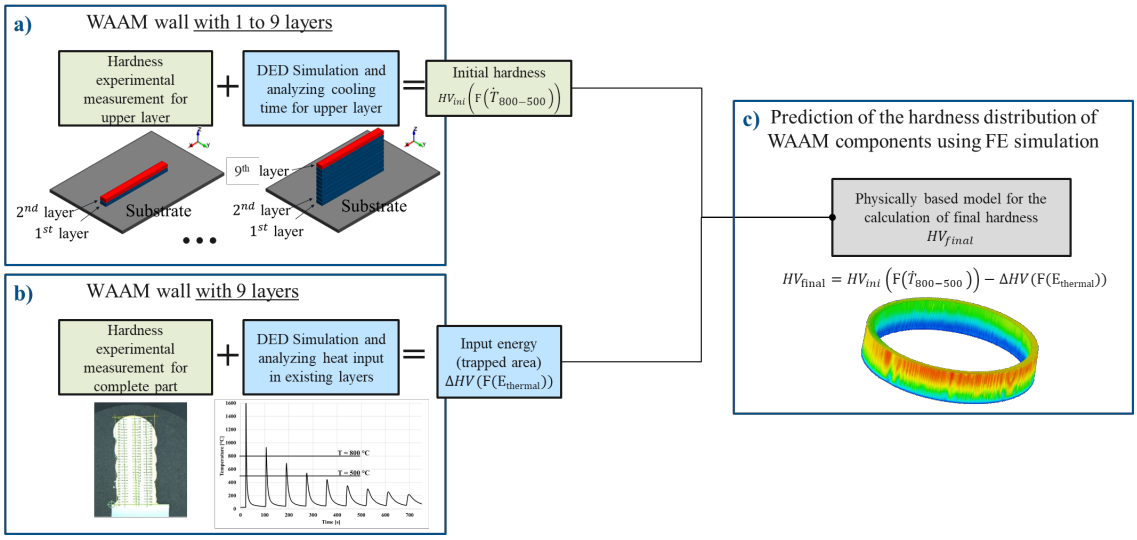

Figure 1: General procedure for developing a physically based model from experimentally measured data (hardness) and simulation data for predicting the hardness distribution of a component after the WAAM process using process simulation.

The hardness distribution in the entire component was experimentally determined. The simulation was then used to analyze the temperature-time curves of the individual layers. As soon as a temperature peak of at least 800 °C was reached for the last time in a layer, the cooling rate between 800 and 500 °C was determined for this peak, and the initial hardness was calculated using the developed model. It is important to note that the selected temperature peak should be the last one that is higher than 800 °C, as the investigated material (AWS A5.18) also undergoes a phase transformation for the last time because of reheating and the resulting hardness depends significantly on the cooling rate between the selected range. All subsequent reheating cycles (by applying additional layers) with maximum temperatures below 800 °C reduce the hardness corresponding to the annealing process. To quantify this thermal energy input, the calculated temperature-time curves are now integrated from the first temperature peak below 800 °C onwards. Fig. 2 presents the procedure schematically for a temperature-time curve.

As the exit hardness of each layer can now be calculated after the final austenitizing and the final hardness after the complete WAAM process has been determined experimentally, the reduction in hardness ΔHV (due to reheating without austenitizing) can be determined and described as a function of the thermal energy. In the present case, the area under the temperature-time curve is assumed to be a measure of the thermal energy. Thus, the temperature-time curve is integrated from the first temperature peak below 800 °C. The change in hardness can therefore be expressed according to the following basic notation.

$$\Delta HV(\mathrm{F}(E_{thermal})) \tag{3}$$

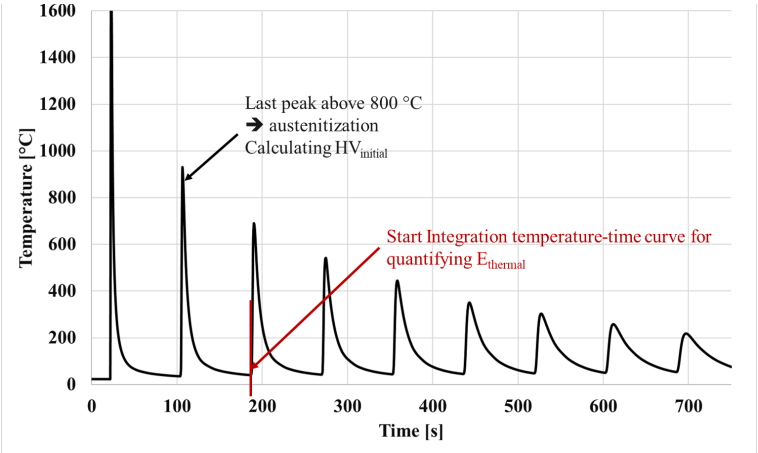

Figure 2: Characteristic evaluation points of a temperature-time curve of a layer.

Experimental setup and Hardness measurement

To analyze the hardness distribution and its development in a welded 9-layer wall, a total of 9 welding experiments were carried out with identical welding parameters, sheet dimensions, and the position of the thermocouples. Conducted experiments differ in the number of welded layers starting with 1 and ending with 9, which is summarized in Table 1.

Table 1. Experiment numbering

Number of experiments	Number of welded layers
1	1
2	2
…	…
9	9

The weld length in each experiment was 300 mm with a fixed break time of 38 s between layers. The welding direction was reversed after each layer to ensure a uniform wall. To avoid temperature effects between experiments, the base plate was cooled to room temperature before starting the next experiment. All welding parameters are summarized in Table 2.

Table 2. WAAM manufacturing parameters

Parameter	Value
Wire diameter	1.2 [mm]
Welding speed	40 [cm/min]
Wire feed	4 [m/min]
Average electrical voltage	14.6 [V]
Average electrical current	144 [A]
Cooling Time between deposition of each layer	38 [s]
Stickout	15 [mm]
Gas / Average Flowrate	M21-ArC-18 / 15 [l/min]

During the welding tests, the temperature was measured at five different locations (Fig. 3) by using K-type wire thermocouples. This is necessary to calibrate the simulation according to the method presented in [8].

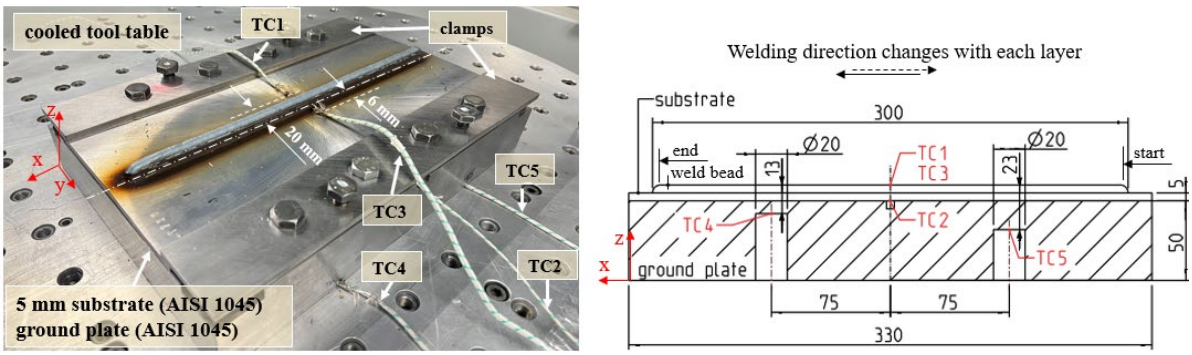

Figure 3. Experimental setup.

For the hardness measurements, samples were cut in the middle and a non-etching sample preparation was carried out. A calibrated DuraScan 70 model from ZwickRoell GmbH & Co KG was used for the Vickers hardness tests. The measurements were carried out in the low force range HV1 with a test load of F = 9.807 N. The hardness of a weld wall was measured in the direction of the weld seam on the line of symmetry, starting from point 0. Fig. 4 presents the idealized welded wall (a), the measured hardness distribution (b), and measure points of the real welded wall (c). A distance between two measuring points equals 0.45 mm, which was determined by dividing the average layer height by 4 so that a layer consists of a total of 5 measuring points. This way a reliable analysis of the hardness distribution within a layer can be performed.

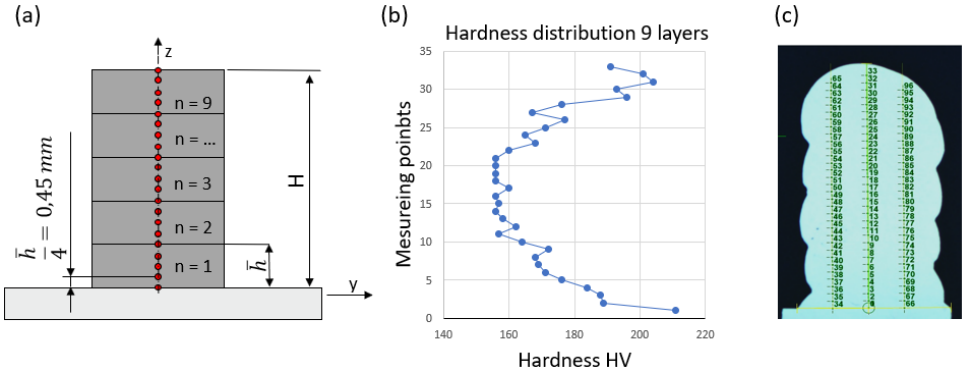

Figure 4. Arrangement of the measuring points in idealized welded wall (a), measured hardness distribution (b), welded wall (c)

Simulation setup and parameters

To reproduce the experimental setup in a digital form, the Simufact. Welding 2021.1 software (Hexagon, Stockholm) is used, where a ground plate, substrate plate, and holding clamps are also included in the developed FE model (Fig 5 a). In a real experiment, the thickness of the successively welded layers differs from each other, which was also considered in the numerical model (Fig 5b).

The density and thermal capacity of the AISI 1045 steel substrate were taken from the literature [6, 7] (Fig. 6 a, b), whereas thermal conductivity was measured with Linseis LFA 1000 Laser Flash test machine (Linseis Messgeräte GmbH, Selb, Germany) (Fig. 6c). Material properties of the AWS A5.18 wire are taken from the Simufact.Welding 2021.1 material database. The applied convective heat transfer parameters were determined in earlier Authors' work [8].

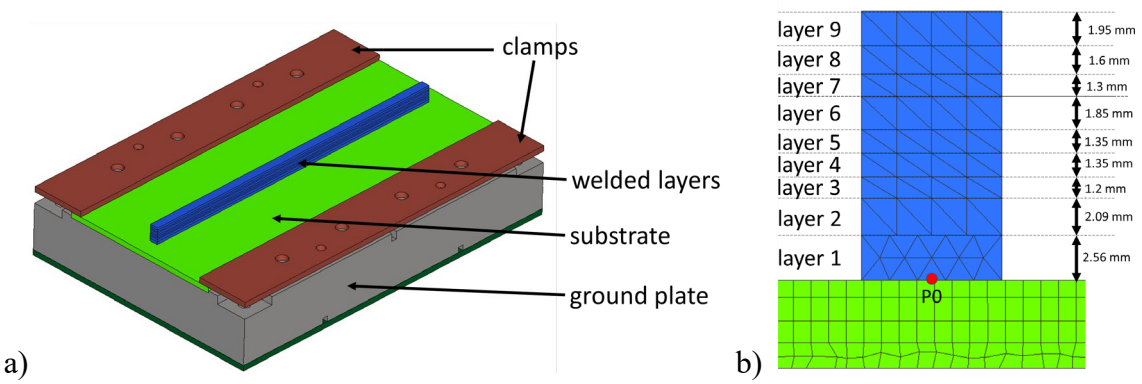

Figure 5. FE model developed in Simufact. Welding software: a) full setup, b) cross-section of the seam.

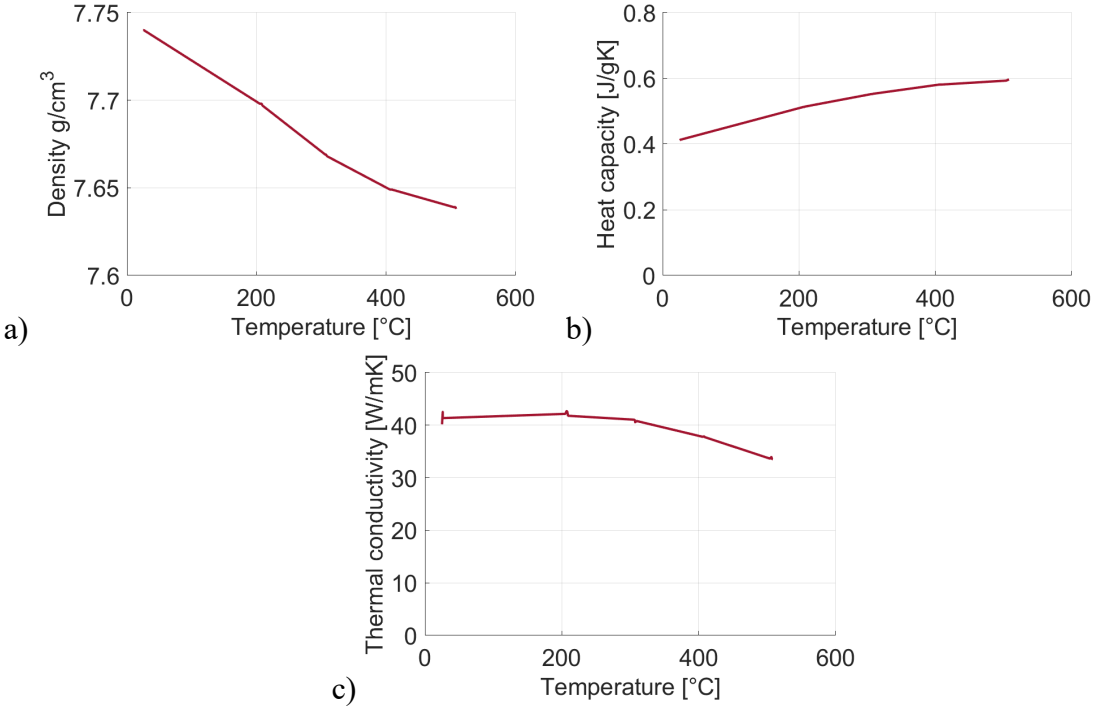

Figure 6. Material properties of AISI 1045 as a function of temperature: a) density [6], b) heat capacity [7], c) thermal conductivity measured by Authors.

Every layer was welded digitally with the same speed (400 mm/min), voltage (14.6 V), and current (144 A) as welding parameters applied during the real experiment. The air temperature and initial temperature of the wire were set to 23°C, the initial temperature of all plates was set to 21.5°C, and arc efficiency was assumed to be 80%. Goldak's heat source model [9] was used to describe the volumetric heat flux density distribution, where a_f, a_r, b, d are parameters related to the shape characteristic of the welding arc. Based on earlier Authors' work [8], two heat source model (HSM) was applied, where the optimization procedure resulted in the following values of the heat source parameters: a_f=4.96 mm, a_r=11.49 mm, b=3 mm, d=2 mm for HSM 1; and a_f=0.1 mm, a_r=0.1 mm, b=0.3 mm, d=0.3 mm for HSM 2.

Initial Hardness as a function of the cooling time

The relationship between the initial hardness and the cooling rate is a crucial factor in the development of the microstructure and mechanical properties of a printed part using WAAM in additive manufacturing. This relationship results from the solidification of the molten material

during the cooling phase, a process in which the cooling rate has a significant influence on the microstructural properties and thus on the hardness of the final product. The complex correlation between faster cooling rates, which result in a harder and finer microstructure, and slower cooling rates, which result in a softer and coarser microstructure, highlights the importance of controlling cooling time as a tactical means of controlling mechanical properties for example.

As mentioned, 9 components with one to nine layers were produced using the WAAM process. The hardness was then measured in the top layer in each case. This procedure means that the resulting hardness is only influenced by the cooling rate and not by any reheating, as no further seam was applied. As already mentioned, the break time until a new layer is welded is constantly 38 s. The numerical process simulation of these nine components with different numbers of layers was then carried out. With the help of the simulation, it is now possible to determine the cooling rate in the seam middle of the uppermost seam (in which the hardness was also measured). This was done for the temperature range between 800 and 500 °C, as the cooling rate in this range has a significant influence on the mechanical properties [10].

Fig. 7 shows the cooling rates and the resulting hardness values for the top layer of the components with 2 to 9 layers. The component with one layer was not evaluated to eliminate the influence of mixing with the base material. It can be seen that the resulting hardness increases with increasing cooling rate. Furthermore, the cooling rate decreases with the number of layers of a component. This is because existing layers have a higher temperature than the base plate and therefore reduce heat conduction. The relationship between the resulting hardness and cooling rate can be described analytically using a quadratic equation with a very high coefficient of determination (see Fig. 7 and Eq. 4).

$$HV_{ini} = 0.0025\dot{T}^2 - 0.0403\dot{T} + 196.34, \quad R^2 = 0.98 \tag{4}$$

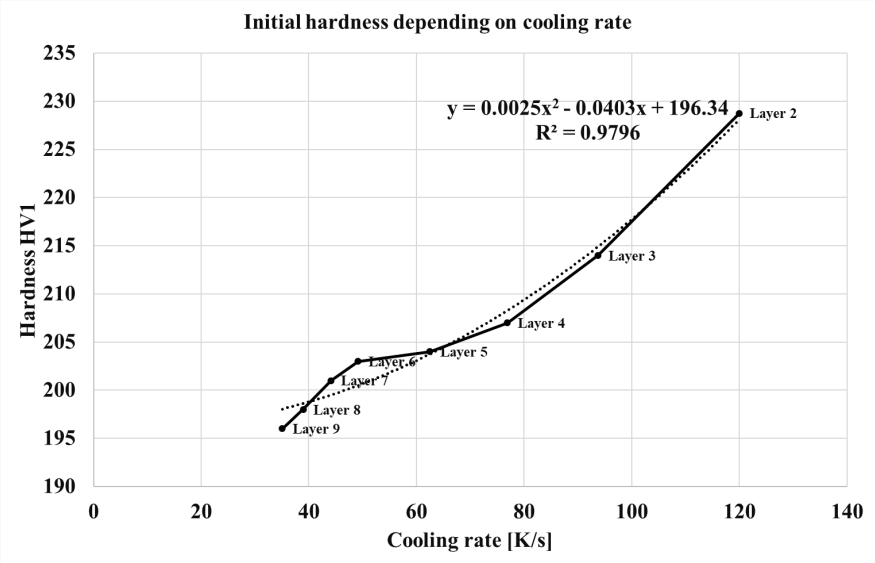

Figure 7. A correlation between initial hardness and cooling rate.

Hardness development during the WAAM process

As the individual layers cool down during the WAAM process and are also reheated as new layers are applied, both cooling and reheating must be considered in the physical-based analytical model. In the context of this work, this is done using the 9-layer wall as an example. Fig. 8 shows a characteristic temperature-time curve for the second layer of the wall with 9 layers. The peak of the temperature at approx. 25 s represents the welding of layer 2, which then cools down to a point in time of approx. 105 s. The layer is then reheated to over 800 °C (including austenitization and

renewed cooling) and then it cools down again. Since this second peak is the last one above 800 °C, the cooling rate between 800 and 500 °C is determined here, and the initial hardness of the $HV_{initial}$ layer is determined using Eq. 4. From a time of 190 s (red line in Fig. 8), it is now assumed that the cyclical reheating corresponds to an annealing treatment, which reduces the hardness. To quantify the amount of thermal energy introduced $E_{thermal}$, the temperature-time curve is integrated from the reheating after the last temperature peak above 800 °C until the end of the process.

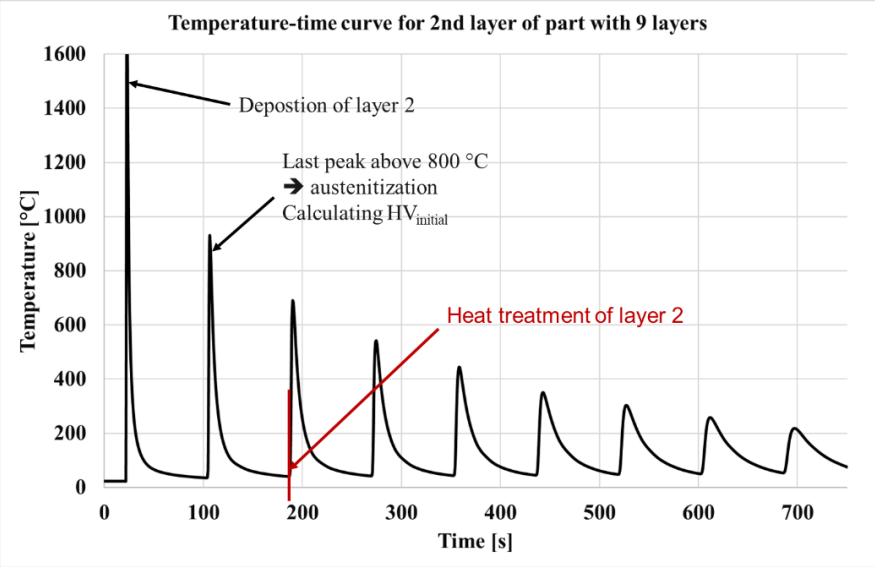

Figure 8. Example of the temperature history at the selected point.

The decrease in hardness (due to reheating) now represents the difference between the measured hardness at the end of the process and the calculated initial hardness (after the last austenitizing) for each layer. This procedure allows Authors to determine a relationship between the hardness difference ΔHV and the area under the temperature-time curve (as a measure of the thermal energy applied). This relationship is shown graphically in Fig. 9.

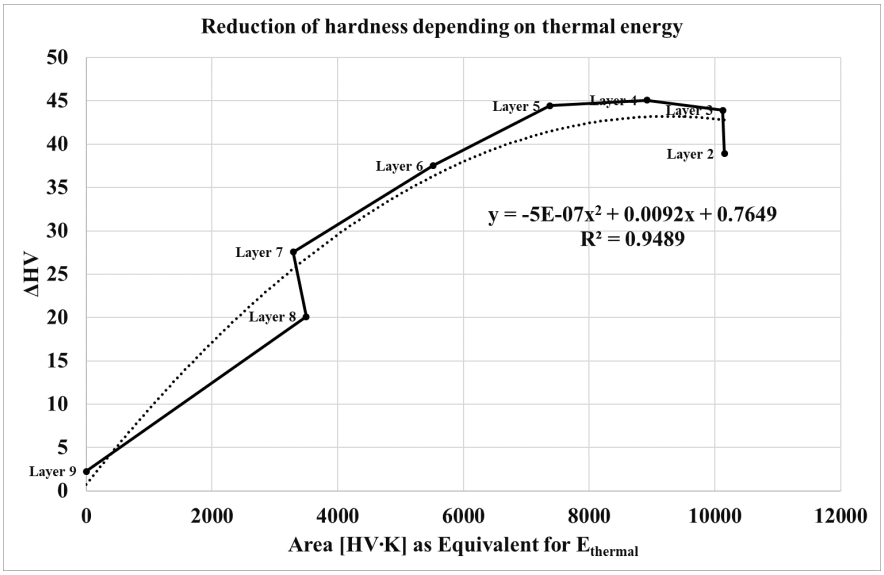

Figure 9. Plot of correlation between reduction of hardness and thermal energy.

It can be seen that the difference in hardness increases with increasing thermal energy input, i.e. the final hardness is reduced to a greater extent. However, from a certain value (from layer 5) an almost stationary range is reached. The relationship between curve area A and decrease in

hardness can also be described analytically with a very high coefficient of determination (see Eq. 5).

$$\Delta HV = -5E-07 \cdot A^2 + 0.0092A + 0.7649, \quad R^2 = 0.95 \tag{5}$$

Using two sub-models from Eq. 4 and 5, the hardness after the WAAM process can now be calculated for each numerically determined temperature-time curve, for the first time considering the cooling-related hardness development and the reduction in hardness due to reheating. In this case, the model was used for the wall with 9 layers. Fig. 10 presents the comparison between the experiment and model as well as the error bar with a deviation of ± 5%. It can be seen that the maximum deviation between the model and simulation is less than 5%.

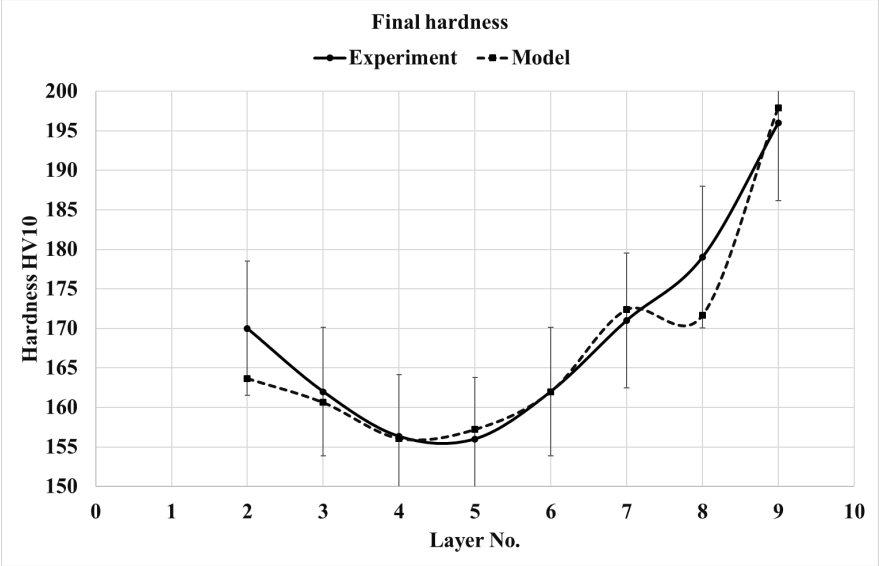

Figure 10. Comparison between experiment and model as well as the error bar with a deviation of ± 5%.

Conclusions

Based on numerical and experimental investigations, the Authors developed a reliable model that predicts the material hardness during and after the WAAM process. This is the first time that an approach has been pursued that considers the development of hardness as a function of both the cooling rate and the energy introduced as a result of reheating by applying additional layers. The analytical model based on physical effects can be integrated into FE systems for the process simulation of WAAM processes using subroutines. This means that the hardness distribution in WAAM-manufactured components can now be reliably predicted using process simulation.

The obtained results prove that:

- As the molten material solidifies during the cooling phase, its microstructure and hardness are influenced by the cooling rate of the material.
- Faster cooling rates can lead to a finer microstructure and thus to a higher hardness, while slower cooling rates can lead to a coarser microstructure and thus to a lower hardness. The formation of hardness can be described analytically as a function of the cooling rate.
- During the process, the hardness of a layer can be reduced by reheating due to the application of further layers. The amount of hardness reduction is essentially dependent on the thermal energy applied and the relationship between hardness reduction and thermal energy can be described analytically.

- By influencing the cooling time, the initial hardness of each printed layer can be effectively controlled, which is a crucial mechanism for adjusting the mechanical properties of the final product.

References

[1] Bai, Y., et al. "Prediction of the evolution of residual stresses in additive manufactured parts using a finite element approach." Finite Elements in Analysis and Design 190 (2022): 103461. https://purls.library.ucf.edu/go/DP0027104

[2] Zhao, Y., et al. "Predicting the mechanical properties of additive manufactured parts using machine learning." Materials Science and Engineering: A 782 (2020): 139329. https://www.sciencedirect.com/science/article/pii/S2238785421006670

[3] Wu, S., et al. "Experimental and numerical investigation of the microstructure and mechanical properties of additive manufactured Ti-6Al-4V." Journal of Materials Science & Technology 38.1 (2022): 1-15. https://www.sciencedirect.com/science/article/abs/pii/S0921509318318008

[4] Zhang, B., et al. "Prediction of the fatigue behavior of additive manufactured parts using a multi-scale approach." International Journal of Fatigue 163 (2022): 107001. https://asmedigitalcollection.asme.org/MSEC/proceedings/MSEC2021/85062/V001T01A015/1115404

[5] Li, Y., et al. "Development of a predictive model for the hardness of additive manufactured AlSi10Mg parts." Journal of Manufacturing Processes 78 (2022): 134-144. https://link.springer.com/article/10.1007/s12666-022-02676-5

[6] M. Hojny, M. Glowacki, Numerical Modelling of Steel Deformation at Extra-High Temperatures, in P. Miidla (ed.), Numerical Modelling, IntechOpen, London, 2012, 10.5772/36562. https://www.intechopen.com/chapters/33087

[7] A. Martinovs, S. Polukoshko, E. Zaicevs, R. Revalds, Laser Hardening Process Optimizations Using FEM, Engineering for Rural Development, 2020, DOI: 10.22616/ERDev2020.19.TF372 https://www.researchgate.net/publication/342412420_LASER_HARDENING_PROCESS_OPTIMIZATION_USING_FEM

[8] J. Szyndler, A. Schmidt, S. Härtel, Determination of welding heat source parameters for FEM simulation based on temperature history and real bead shape. Materials Research Proceedings 28 (2023) 159-168. https://doi.org/10.21741/9781644902479-18

[9] J. Goldak, A.P. Chakravarti, M. Bibby, A new finite element model for welding heat sources, Metallurgical Transactions B, 15 (1984) 299-305. https://link.springer.com/article/10.1007/BF02667333

[10] M. Mician, D. Harmaniak, F. Novy, J. Winczek, J. Moravec, L. Trsko, Effect of the t8/5 cooling time on the properties of S960MC steel in the HAZ of welded joints evaluated by thermal physical simulation. Metals (2020) 10 (2) 229. https://doi.org/10.3390/met10020229